Implementation of a Cubature Kalman Filter for Power Estimation of Non-ideal Constant Power Loads in a DC Microgrid

SHIRIN YOUSEFIZADEH[1a], NAVID VAFAMAND[2b], JAN DIMON BENDTSEN[1c], MOHAMMAD HASSAN KHOOBAN[2d], FREDE BLAABJERG[2e]
[1]Electronic Systems Department, Aalborg University, 9220 Aalborg, DENMARK
[2]Energy Technology Department, Aalborg University, 9220 Aalborg, DENMARK
[a)]shy@es.aau.dk, [b)]nav@et.aau.dk, [c)]dimon@es.aau.dk, [d)]kho@et.aau.dk, [e)]fbl@et.aau.dk

Abstract: - DC microgrids (MG) involve the integration of power electronic loads, which might behave as constant power loads (CPL). CPLs often degrade system stability due to their negative impedance characteristics. To maintain the voltage stability and safe operation of DC MGs, eliminating the undesired behavior of CPLs is a necessity. This aim requires the instantaneous power value of the time-varying uncertain CPLs. Since the integration of current sensors in DC MGs is costly and inefficient, estimation methods should be used to obtain the spontaneous power of CPLs. In this paper, a 3rd degree cubature Kalman filter (CKF) is developed to estimate the power of the CPLs alongside estimation of CPLs' and source's currents in a DC MG. By considering the CPLs powers as artificial states and augmenting them into the system states, not only the DC MG states but also the unknown values of the CPLs powers may be estimated. The proposed estimator is tested on a DC MG that feeds one CPL. The experimental results show that the proposed CKF is able to estimate instantaneous power consumption of the CPL as well as source and load currents.

Key-Words: - Estimation, Cubature Kalman filter, DC microgrid, Non-ideal Constant power load

Nomenclature

ACRONYMS	
CPL	Constant Power Load
MG	Microgrid
CKF	Cubature Kalman Filter
EKF	Extended Kalman Filter
ESS	Energy Storage System
DC MG PARAMETERS	
i_{Lj}	Current of the inductor in the j-th CPL
v_{Cj}	Voltage of the capacitor in the j-th CPL
P_j	The power of the j-th CPL
r_j	Resistance of the j-th filter connected to the j-th CPL
L_j	Inductance of the j-th filter connected to the j-th CPL
C_j	Capacitance of the j-th filter connected to the j-th CPL
r_s	Resistance of the filter connected to the DC source
L_s	Inductance of the filter connected to the DC source
C_s	Capacitance of the filter connected to the DC source
V_{dc}	Voltage of the DC source
i_{es}	Injecting current of the ESS
CKF PARAMETERS	
$\mathcal{P}_{k\|j}$	Covariance of the states at sampling instant k based on the information up to the sampling instant j
$X_{i,k-1\|k-1}$	i-th cubature point at sampling instant $k-1$ based on the information up to the sampling instant $k-1$
$X^*_{i,k\|k-1}$	i-th propagated cubature point by the system model at sampling instant k based on the information up to the sampling instant $k-1$
$\hat{x}_{k\|j}$	Estimated states at sampling instant k based on the information up to the sampling instant j
$Y_{i,k\|k-1}$	i-th propagated cubature point by the measurement model at sampling instant k based on the information up to the sampling instant $k-1$
$\hat{y}_{k\|k-1}$	Estimated measurements at sampling instant k based on the information up to the sampling instant $k-1$
$\mathcal{P}_{xy,k\|k-1}$	Estimated cross-covariance matrix at sampling instant k based on the information up to the sampling instant $k-1$
K_k	Kalman gain at sampling instant k

1 Introduction

The growing use of renewable energy sources such as fuel cells [1], wind turbines [2], and

photovoltaic systems [3] in power electronic systems has reinforced a trend toward microgrids (MG). Microgrids enable electric power distribution from renewable energy sources. The two types of MGs are alternating-current (AC) and direct-current (DC) MGs [4]. Because of the AC MGs interfacing with utility grids, AC MGs have been studied since 2000s [4]. However, many renewable energy sources and recent loads have DC interface and due to the advantages of DC MGs over AC MGs there is a tendency toward using DC MGs [5]. Some of these advantages are natural interface with renewable energy sources [6], power loss reduction in AC/DC power conversion [7], removing frequency control problems, improving power quality, decreasing the space and weight of transformers [5], and improving fault reconfigurability. Therefore, DC MGs are increasingly used in different applications such as electric vehicles [8], aircraft [9], ships [10], etc. A DC MG has several challenging stability and performance issues. These challenges primarily arise due to the vast interactions of power electronic converters, which might create constant power loads (CPLs). CPLs are generated by strict controlling of power electric converter loads. The incremental negative impedance of CPLs, can result in severe stability issues for the DC MG or even destabilize the overall system. Thus, minimizing the undesired effect of the CPLs is a necessity to have a successful control of the DC MGs.

Several strategies are proposed to mitigate the destructive effects of CPLs in DC/DC power electronic converters. Two basic strategies are passive damping and active damping approaches [11]. Passive damping includes adding damping resistors to the filters. Even though this approach is simple and effective, it causes a lot of dissipation. Active damping involves modifying the control loop, which acts like a virtual resistor [11]. Active damping approaches are commensurate with injecting power to the CPLs to stabilize the system, which comprises the load performance [12]. In addition, these active damping approaches, which are based on small-signal models, can ensure system stability only close to the operating point. Therefore, these linear control methods are not useful in the case of occurrence of large variations in the system [12]. Several nonlinear control approaches have been investigated in order to address the stability problems with the DC MGs containing CPLs [13] and mitigating the undesired behavior of CPLs in such systems [14], [15], [12]. Nonetheless, the common assumption in the aforementioned methods is that the CPLs are assumed to be ideal. An ideal CPL is assumed to consume a constant power regardless of the supply voltage value. Yet, in practice, the MGs feed uncertain and/or time-varying CPLs, known as non-ideal CPLs. A few papers have studied the effect of non-ideal CPLs on the system stability [16]–[18]. Even though the proposed approaches in [16]–[18] provide stability analysis and robust controller design, their common assumption is the boundedness of power uncertainty by a pre-known limit. To overcome the considered limit on CPLs powers uncertainty, the instantaneous power value of the time-varying uncertain CPLs is necessary. The CPLs powers can be obtained by employing current and voltage sensors. The current sensor must be installed in series with the CPLs, which not only increases the output impedance but also degrades ripple filtering effect [12]. In addition, installing extra sensors increases system complexity, and increases buying, installing and repairing costs. Therefore, current sensors installation should be replaced with the estimation methods to estimate the CPLs currents and powers.

Two basic approaches for unknown parameter estimation are deterministic observers and stochastic estimators. In deterministic observers, the unknown parameters are treated as disturbances. The equivalent disturbance is then estimated by modifying the difference between the estimated output and the output of the nominal response model [19]. However, measurement noises may degrade the deterministic observers' performance [20]. Kalman filters have been proved to be optimal against noise effects [21]. The extended Kalman filter (EKF) applies the Kalman filter to nonlinear systems by linearizing the system model. The EKF exhibits a poor performance for highly nonlinear dynamic systems [22]. Bayesian sampling methods are alternatives to the EKF. These methods are divided into random sampling and deterministic sampling [23]. Random sampling methods involve in high computational burden, which makes them inappropriate for practical applications. Among deterministic sampling methods, cubature Kalman filters (CKF) possess various advantages, such as accuracy, lower computational effort, and more numerical stability [23] and have therefore attracted interest in the research community of late.

In this paper, to eliminate the undesired effects of CPLs in DC MG operation, a cost-effective 3rd degree CKF algorithm is developed to employ a joint estimation problem to estimate not only DC MG's states but also CPLs powers. The main contribution of this paper is employing the developed CKF to estimate the CPLs instantaneous powers and currents, and the current of the source.

To achieve this goal, the CPLs powers are augmented into the state vector of the system as virtual states. Since the CKF is robust against the system uncertainties, unmodeled dynamics, and noisy measurements, the proposed technique is reliable and economical in practice. The developed CKF is then applied to a DC MG, which is connected to an uncertain time-varying CPL. The efficacy of our proposed method is verified by laboratory experiments.

The outline of this paper is as follows. The modeling of the DC MG is provided in section II. In section III, the developed CKF algorithm for unknown power estimation is presented. To investigate the performance of the proposed estimator, illustrative experimental results are presented in sections IV. Finally, Section V concludes the paper.

2 DC Microgrid Dynamic

A typical DC MG, which comprises several CPLs, is shown in Fig. 1, and its circuit diagram is shown in Fig. 2. The system shown in Fig. 2 consists of Q CPLs and 1 energy storage system (ESS). By employing the Kirchhoff's current and voltage laws, the dynamic model of the j-th CPL is obtained as

$$\begin{cases} \dot{x}_j = A_j x_j + d_j P_j + A_{js} x_s \\ y_j = h_j x_j \end{cases} \tag{1}$$

where P_j is the load power, $x_j = \begin{bmatrix} i_{Lj} & v_{Cj} \end{bmatrix}^T$ is the j-th CPL's state vector, and

$$A_j = \begin{bmatrix} -\frac{r_{Lj}}{L_j} & -\frac{1}{L_j} \\ \frac{1}{C_j} & 0 \end{bmatrix}, d_j = \begin{bmatrix} 0 \\ \frac{-1}{C_j v_{cj}} \end{bmatrix}, A_{js} = \begin{bmatrix} 0 & \frac{1}{L_j} \\ 0 & 0 \end{bmatrix}, \tag{2}$$

$$h_j = [0 \quad 1]$$

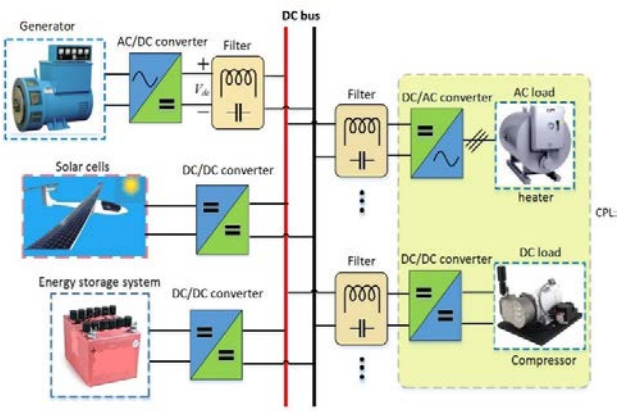

Fig. 1. Illustration of a DC MG.

As for CPLs, the dynamic model of the ESS is obtained as

$$\begin{cases} \dot{x}_s = A_s x_s + b_s V_{dc} + b_{es} i_{es} + \Sigma_{j=1}^{Q} A_{cn} x_j \\ y_s = h_s x_s \end{cases} \tag{3}$$

where i_{es} is the ESS injection current, $x_s = [i_{Ls} \;\; v_{Cs}]^T$ is the ESS state vector, and

$$A_s = \begin{bmatrix} -\frac{r_s}{L_s} & -\frac{1}{L_s} \\ \frac{1}{C_s} & 0 \end{bmatrix}, \; b_s = \begin{bmatrix} \frac{1}{L_s} \\ 0 \end{bmatrix}, \; h_s = [0 \quad 1],$$

$$A_{cn} = \begin{bmatrix} 0 & 0 \\ \frac{-1}{C_s} & 0 \end{bmatrix}, \qquad b_{es} = \begin{bmatrix} 0 \\ -\frac{1}{C_s} \end{bmatrix} \tag{4}$$

By augmenting the CPLs and the source state vectors, the overall dynamic model of the DC MG is obtained as [24]

$$\begin{cases} \dot{X} = \overline{A} X + \overline{D} P + \overline{B_{es}} i_{es} + \overline{B_s} V_{dc} \\ Y = \overline{H} X \end{cases} \tag{5}$$

where $X = \begin{bmatrix} x_1^T & x_2^T & \dots & x_Q^T & x_s^T \end{bmatrix}^T$, $P = \begin{bmatrix} P_1, \dots, P_Q \end{bmatrix}^T$, and

$$\overline{A} = \begin{bmatrix} A_1 & 0 & \dots & 0 & A_{1s} \\ 0 & A_2 & \cdots & 0 & A_{2s} \\ \vdots & \vdots & \ddots & \vdots & \vdots \\ 0 & 0 & \cdots & A_Q & A_{Qs} \\ A_{cn} & A_{cn} & \cdots & A_{cn} & A_s \end{bmatrix}, \overline{B_{es}} = \begin{bmatrix} 0 \\ \vdots \\ 0 \\ b_{es} \end{bmatrix},$$

$$\overline{B_s} = \begin{bmatrix} 0 \\ \vdots \\ 0 \\ b_s \end{bmatrix}, \overline{D} = \begin{bmatrix} d_1 & 0 & \dots & 0 \\ 0 & d_2 & \cdots & 0 \\ \vdots & \vdots & \ddots & \vdots \\ 0 & 0 & \cdots & d_Q \\ 0 & 0 & \cdots & 0 \end{bmatrix}, \tag{6}$$

$$\overline{H} = \begin{bmatrix} 0 & 1 & 0 & 0 & \dots & 0 \\ 0 & 0 & 0 & 1 & \dots & 0 \\ \vdots & \vdots & \vdots & \vdots & \vdots & \vdots \\ 0 & 0 & 0 & 0 & \dots & 1 \end{bmatrix}$$

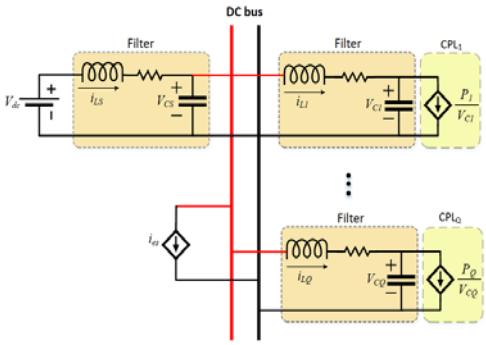

Fig. 2. A simplified illustration of the DC MG shown in Fig. 1 with Q CPLs, where $i_{CPL_j} = \frac{P_j}{V_{Cj}}$.

In the following, the goal is to estimate the powers of the CPLs and the inductor currents alongside noise mitigation.

3 CPL Power Estimatiom by Cubature Kalman Filter

This section presents the design procedure of the developed 3rd degree CKF to estimate the unknown power of CPLs alongside estimation of the source and CPL currents. To this aim, the system state vector is augmented by the unknown CPL power vector [4]. Thereby, the augmented state vector is defined as

$$\dot{z} = \begin{bmatrix} \dot{X} \\ \dot{P} \end{bmatrix} \tag{7}$$

Since the P dynamic is unknown, it is considered as $\dot{P}_j = 0$ for $j = 1, \dots, Q$. Then, the augmented state-space model for the system is

$$\dot{x} = \begin{bmatrix} \overline{A}X + \overline{D}P + \overline{B_{es}} i_{es} + \overline{B_s} V_{dc} \\ \mathbf{0} \end{bmatrix} = f(x, i_{es}) \tag{8}$$

Considering (9), the system measurements are described as

$$y = [\overline{H} | \mathbf{0}] \begin{bmatrix} X \\ P_j \end{bmatrix} \tag{9}$$

Putting (11), (12) together and considering system and measurement noises, w and v, respectively, yields

$$\begin{cases} \dot{x} = f(x, i_{es}) + w \\ y = Hx + v \end{cases} \tag{10}$$

where w and v are assumed white and Gaussian with covariance matrices Q and R, respectively. The obtained state-space model can be discretized using the forward Euler method as

$$\begin{cases} x_{k+1} = x_k + T_s f(x_k, i_{esk}) + w_k \\ y_k = Hx_k + v_k \end{cases} \tag{11}$$

The 3rd degree CKF algorithm is done by recursively performing time update and measurement update. After convergence of the CPL, the last element of $\hat{x}_{k|k}$ is the estimated power of the CPL. The CKF steps are as follows [25]:

- **Time Update**

1. Factorizing $\mathcal{P}_{k-1|k-1}$ by Cholesky decomposition

$$\mathcal{P}_{k-1|k-1} = S_{k-1|k-1} S_{k-1|k-1}^T \tag{12}$$

2. Calculating cubature points for $i = 1, \dots 2n$

$$X_{i,k-1|k-1} = S_{k-1|k-1} \zeta_i + \hat{x}_{k-1|k-1} \tag{13}$$

3. Propagating cubature points by the nonlinear model

$$X^*_{i,k|k-1} = F(X_{i,k-1|k-1}, i_{es,k-1}) \tag{14}$$

4. Estimating the predicted states

$$\hat{x}_{k|\,k-1} = \frac{1}{2n} \Sigma_{i=1}^{2n} X^*_{i,k|\,k-1} \tag{15}$$

5. Estimating the predicted covariance of the states

$$\mathcal{P}_{k|k-1} = \frac{1}{2n} \Sigma_{i=1}^{2n} \left(X^*_{i,k|k-1} - \hat{x}_{k|k-1}\right) \left(X^*_{i,k|k-1} - \hat{x}_{k|k-1}\right)^T + Q_{k-1} \tag{16}$$

- **Measurement Update**

1. Factorizing $\mathcal{P}_{k|k-1}$ by Cholesky decomposition

$$\mathcal{P}_{k|k-1} = S_{k|k-1} S_{k|k-1}^T \tag{17}$$

2. Calculating cubature points for $i = 1, \dots 2n$

$$X_{i,k-1|k-1} = S_{k|k-1} \zeta_i + \hat{x}_{k|k-1} \quad for \quad i = 1, \dots 2n \tag{18}$$

3. Propagating cubature points by the measurement model

$$Y_{i,k|\,k-1} = h(X_{i,k|k-1}, i_{es,k}) \tag{19}$$

4. Estimating the predicted measurements

$$\hat{y}_{k|\,k-1} = \frac{1}{2n} \Sigma_{i=1}^{2n} Y_{i,k|\,k-1} \tag{20}$$

5. Estimating the auto covariance matrix

$$\mathcal{P}_{yy,k|k-1} = \frac{1}{2n} \Sigma_{i=1}^{2n} \left(Y_{i,k|\,k-1} - \hat{y}_{k|k-1}\right) \left(Y_{i,k|k-1} - \hat{y}_{k|k-1}\right)^T + R_k \tag{21}$$

6. Estimating the cross-covariance matrix

$$\mathcal{P}_{xy,k|k-1} = \frac{1}{2n}\Sigma_{i=1}^{2n}\left(X_{i,k|\,k-1} - \hat{x}_{k|k-1}\right) \left(Y_{i,k|k-1} - \hat{y}_{k|k-1}\right)^{T} + R_k \quad (22)$$

7. Estimating the Kalman gain

$$K_k = \mathcal{P}_{xy,k|k}\,\mathcal{P}_{yy,k|\,k-1}^{-1} \quad (23)$$

8. Estimate the updated states

$$\hat{x}_{k|k} = \hat{x}_{k|k-1} + K_k\left(y_k - \hat{y}_{k|k}\right) \quad (24)$$

9. Estimating the covariance of the states

$$\mathcal{P}_{k|k} = \mathcal{P}_{k|k-1} + K_k\mathcal{P}_{yy,k|k}K_k^T \quad (25)$$

where R_k, Q_{k-1} are the measurement covariance matrix and the process noise covariance matrix, respectively. By the means of the CKF and having $v_{C,j}, v_{C,s}$ measurements, the estimations of P_j for $j = 1, \dots, Q$ are achieved by being extracted from the state vector x.

4 Experimental Results

To verify the effectiveness of the proposed nonlinear observer, experimental results are provided in this section. The experimental testbed is shown in Fig. 3.

It is assumed that all voltages and currents are real. The MG parameters used in the simulations are listed in Table I.

Table 1. Parameters For the DC MG with One CPL.

$r_1 = 1.1\ \Omega$	$v_{C0,1} = 196.64$	$C_s = 500\ \mu F$
$L_1 = 39.5\ mH$	$V_{dc} = 200\ V$	$P_1 = 300\ W$
$C_1 = 500\ \mu F$	$r_s = 1.1\ \Omega$	$L_s = 39.5\ mH$

The simulation is done by choosing the initial condition of $X = [1 \quad 210 \quad 1 \quad 200 \quad 350\ ]^T$. The values for measurement covariance matrix and the process noise covariance matrix are as:

$$R = diag(10^{-3}, 10^{-3}) \quad Q = diag(10^{-2}, 10^{-5}, 10^{-2}, 10^{-5}, 10^{-2}) \quad (26)$$

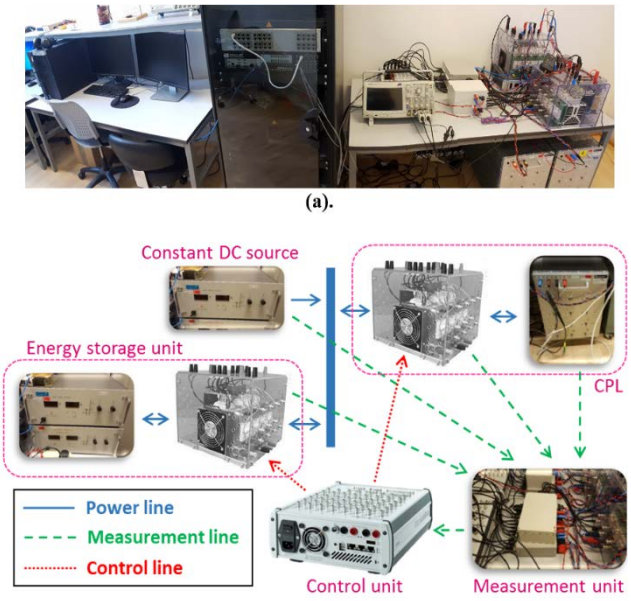

Fig. 3. (a). The experimental setup. (b). The simplified implementation configuration.

The initial value of the states' error covariance matrix is chosen as:

$$p_0 = diag(1,1,1,1,10^2) \quad (27)$$

To show the effectiveness of the proposed nonlinear filter, two scenarios are provided. In both scenarios, the value of the CPL power should vary within a specific interval to assure the stability of the DC MG. In the first scenario, step decreases and increases in the CPL power, P_1, is considered. These prompt changes can occur in practice when the characteristics of the connected loads to the inverters, which behave as CPLs, changes promptly. In the second scenario, the CPL power varies slowly. In practice, the slow variation of P occurrs because the efficiency of converters is not constant in practice and the controller of the converters has a limited bandwidth. In the following, the experimental results for both scenarios is presented. The time scale in all figures is $0.6\ sec$.

Scenario 1 (Stepwise varying P_1): In this scenario, the CPL power increases and decreases promptly at some moments. By applying the developed CKF, the currents and voltages of the CPL filters and the DC source filter, as well as the CPL power are estimated. Fig. 4 shows the actual values of the system states alongside their estimations by employing the CKF.

As can be seen in Figs. 4, the proposed filter can estimate the CPL power fast and accurately. In addition, it can be seen that in the moments of occurring the prompt changes in the CPL power, an error is produced in its estimation. Meanwhile, the CKF is able to treat these sudden changes effectively and retrieve the CPL power estimation to its actual value. A short time after the fats changes in the CPL power, since the power is constant, the estimation error of the states becomes zero.

Scenario 2 (periodic slowly varying P_1): In this scenario, the CPL power changes slowly. For the simulation, the CPL power value changes as $P_1 = 200(1 + \sin(5t) + 0.5\cos(7t))$. Fig. 5 shows the actual values of the system states alongside their estimations by employing the CKF.

As can be seen in Figs. 5, the suggested observer can estimate the value of the CPL power effectively. Comparing to the Scenario 1, In the case of continuously varying power, the proposed CKF can capture the varying behavior of the DC MG more precise and results in a smaller estimation error.

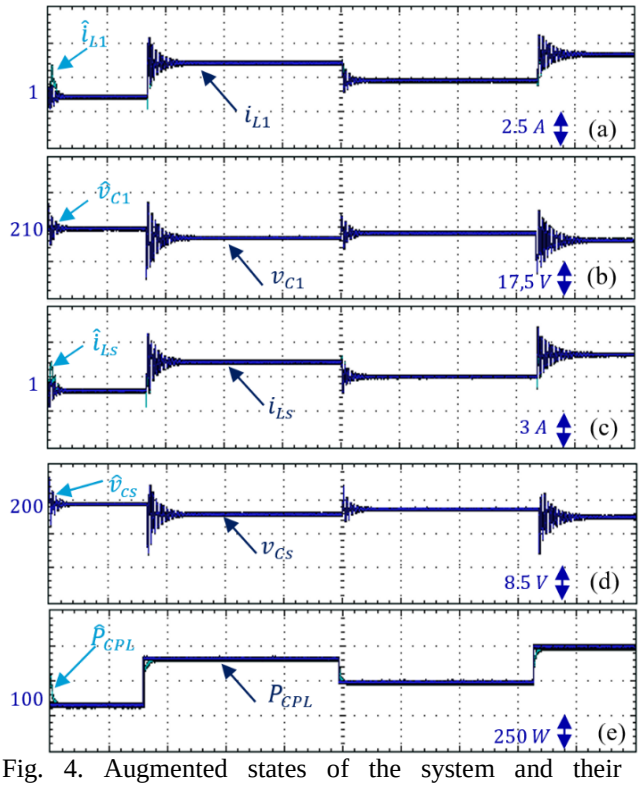

Fig. 4. Augmented states of the system and their estimation for Scenario 1.

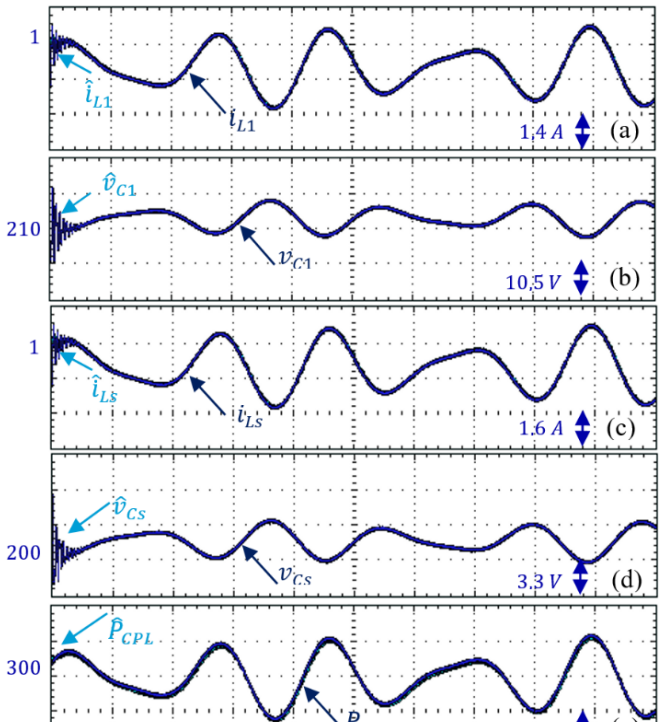

Fig. 5. Augmented states of the system and their estimation for Scenario 2.

5 Conclusion

This paper aimed to rapidly estimate values of the CPL power to be used later on for stability control and safe operation of the DC MGs. To do this, first, the CPL powers are augmented in the system state vector, and then a cubature Kalman filter is developed to estimate the CPLs powers alongside the estimation of the system's currents. To illustrate the effectiveness of the proposed power estimation, the real-time implementation is performed on a DC MG that feeds one CPL. Then, two scenarios including fast changes and slow changes in the CPL power are considered. The real-time experimental results showed the ability of the proposed observer in estimating the instantaneous power of the CPLs used in the DC MGs for both scenarios of sudden and continuous changes of the CPL power. Future work could be using other types of stochastic and deterministic observers and comparing the estimation results with the estimations using the CKF. The other possible future work could be tuning the CKF parameters using optimization techniques.

References:

[1] Y. Han, W. Chen, Q. Li, H. Yang, F. Zare, and Y. Zheng, "Two-level energy management strategy for PV-Fuel cell-battery-based DC microgrid," *Int. J. Hydrog. Energy*, May 2018.

[2] D. Pavković, M. Cipek, M. Hrgetić, and A. Sedić, "Modeling, parameterization and damping optimum-based control system design for an airborne wind energy ground station power plant," *Energy Convers. Manag.*, vol. 164, pp. 262–276, May 2018.

[3] H. Islam *et al.*, "Performance Evaluation of Maximum Power Point Tracking Approaches and Photovoltaic Systems," *Energies*, vol. 11, no. 2, p. 365, Feb. 2018.

[4] A. Gupta, S. Doolla, and K. Chatterjee, "Hybrid AC-DC Microgrid: Systematic Evaluation of Control Strategies," *IEEE Trans. Smart Grid*, vol. 9, no. 4, pp. 3830–3843, Jul. 2018.

[5] Z. Jin, G. Sulligoi, R. Cuzner, L. Meng, J. C. Vasquez, and J. M. Guerrero, "Next-Generation Shipboard DC Power System: Introduction Smart Grid and dc Microgrid Technologies into Maritime Electrical Netowrks," *IEEE Electrification Mag.*, vol. 4, no. 2, pp. 45–57, Jun. 2016.

[6] H. Kakigano, Y. Miura, and T. Ise, "Low-voltage bipolar-type DC microgrid for super high quality distribution," *IEEE Trans. Power Electron.*, vol. 25, no. 12, pp. 3066–3075, 2010.

[7] L. Ding, Q. Han, L. Y. Wang, and E. Sindi, "Distributed Cooperative Optimal Control of DC Microgrids With Communication Delays," *IEEE Trans. Ind. Inform.*, vol. 14, no. 9, pp. 3924–3935, Sep. 2018.

[8] *Modern Electric, Hybrid Electric, and Fuel Cell Vehicles, Third Edition*. CRC Press, 2018.

[9] S. Yousefizadeh, J. D. Bendtsen, N. Vafamand, M. H. Khooban, T. Dragicevic, and F. Blaabjerg, "Tracking Control for a DC Microgrid Feeding Uncertain Loads in More Electric Aircraft: Adaptive Backstepping Approach," *IEEE Trans. Ind. Electron.*, 2018.

[10] Z. Jin, L. Meng, J. M. Guerrero, and R. Han, "Hierarchical Control Design for a Shipboard Power System With DC Distribution and Energy Storage Aboard Future More-Electric Ships," *IEEE Trans. Ind. Inform.*, vol. 14, no. 2, pp. 703–714, Feb. 2018.

[11] A. M. Rahimi and A. Emadi, "Active Damping in DC/DC Power Electronic Converters: A Novel Method to Overcome the Problems of Constant Power Loads," *IEEE Trans. Ind. Electron.*, vol. 56, no. 5, pp. 1428–1439, May 2009.

[12] Q. Xu, C. Zhang, C. Wen, and P. Wang, "A Novel Composite Nonlinear Controller for Stabilization of Constant Power Load in DC Microgrid," *IEEE Trans. Smart Grid*, In press, 2018.

[13] D. Marx, P. Magne, B. Nahid-Mobarakeh, S. Pierfederici, and B. Davat, "Large Signal Stability Analysis Tools in DC Power Systems With Constant Power Loads and Variable Power Loads-A Review," *IEEE Trans. Power Electron.*, vol. 27, no. 4, pp. 1773–1787, Apr. 2012.

[14] P. Magne, B. Nahid-Mobarakeh, and S. Pierfederici, "General Active Global Stabilization of Multiloads DC-Power Networks," *IEEE Trans. Power Electron.*, vol. 27, no. 4, pp. 1788–1798, Apr. 2012.

[15] G. Sulligoi, D. Bosich, G. Giadrossi, L. Zhu, M. Cupelli, and A. Monti, "Multiconverter Medium Voltage DC Power Systems on Ships: Constant-Power Loads Instability Solution Using Linearization via State Feedback Control," *IEEE Trans. Smart Grid*, vol. 5, no. 5, pp. 2543–2552, Sep. 2014.

[16] S. Sumsurooah, M. Odavic, and S. Bozhko, "μ Approach to Robust Stability Domains in the Space of Parametric Uncertainties for a Power System With Ideal CPL," *IEEE Trans. Power Electron.*, vol. 33, no. 1, pp. 833–844, Jan. 2018.

[17] J. Liu, W. Zhang, and G. Rizzoni, "Robust Stability Analysis of DC Microgrids With Constant Power Loads," *IEEE Trans. Power Syst.*, vol. 33, no. 1, pp. 851–860, Jan. 2018.

[18] E. Hossain, "Addressing Instability Issues in Microgrids Caused By Constant Power Loads Using Energy Storage Systems," Theses and Dissertations, University of Wisconsin-Milwaukee, Wisconsin, United States, 2016.

[19] K. S. Eom, I. H. Suh, W. K. Chung, and S.-R. Oh, "Disturbance observer based force control of robot manipulator without force sensor," in *IEEE International Conference on Robotics and Automation*, vol. 4, pp. 3012–3017, 1998.

[20] C. Mitsantisuk, K. Ohishi, S. Urushihara, and S. Katsura, "Kalman filter-based disturbance observer and its applications to sensorless force control," *Adv. Robot.*, vol. 25, no. 3–4, pp. 335–353, 2011.

[21] D. Simon, *Optimal state estimation: Kalman, H∞ and nonlinear approaches*. Hoboken, N.J: Wiley-Interscience, 2006.

[22] N. Vafamand, S. Yousefizadeh, M. H. Khooban, T. Dragičević, and J. D. Bendtsen, "EKF for Power Estimation of Uncertain Time-varying CPLs in DC Shipboard MGs," presented at the 44th Annual Conference of

the IEEE Industrial Electronics Society (IECON 2018), Washington DC, USA, 2018.

[23] Z. Xin-Chun and G. Cheng-Jun, "Cubature Kalman filters: Derivation and extension," *Chin. Phys. B*, vol. 22, no. 12, p. 128401, 2013.

[24] S. Yousefizadeh, N. Vafamand, J. D. Bendtsen, M. H. Khooban, F. Blaabjerg, and T. Dragičević, "Online Power Estimation of non-ideal CPLs in Shipboard DC MGs Using Cubature Kalman Filter," presented at the 2nd European Conference on Electrical Engineering & Computer Science, Bern, Switzerland, 2018.

[25] H. Jianjun, Z. Jiali, and J. Feng, "A CKF based spatial alignment of radar and infrared sensors," in *IEEE International Conference on Signal Processing (ICSP)*, pp. 2386–2390, 2010.